

# Introduction to Monte Carlo Methods

*Helmut G. Katzgraber*

*Department of Physics and Astronomy, Texas A&M University  
College Station, Texas 77843-4242 USA*

*Theoretische Physik, ETH Zurich  
CH-8093 Zurich, Switzerland*

**Abstract.** Monte Carlo methods play an important role in scientific computation, especially when problems have a vast phase space. In this lecture an introduction to the Monte Carlo method is given. Concepts such as Markov chains, detailed balance, critical slowing down, and ergodicity, as well as the Metropolis algorithm are explained. The Monte Carlo method is illustrated by numerically studying the critical behavior of the two-dimensional Ising ferromagnet using finite-size scaling methods. In addition, advanced Monte Carlo methods are described (e.g., the Wolff cluster algorithm and parallel tempering Monte Carlo) and illustrated with nontrivial models from the physics of glassy systems. Finally, we outline an approach to study rare events using a Monte Carlo sampling with a guiding function.

## Contents

---

<b>1</b>	<b>Introduction</b> . . . . .	<b>2</b>
<b>2</b>	<b>Monte Carlo integration</b> . . . . .	<b>3</b>
2.1	Traditional integration schemes . . . . .	3
2.2	Simple and Markov-chain sampling . . . . .	4
2.3	Importance sampling . . . . .	8
<b>3</b>	<b>Interlude: Statistical mechanics</b> . . . . .	<b>9</b>
3.1	Simple toy model: The Ising model . . . . .	9
3.2	Statistical physics in a nutshell . . . . .	10

<b>4</b>	<b>Monte Carlo simulations in statistical physics . . . . .</b>	<b>12</b>
4.1	Metropolis algorithm . . . . .	13
4.2	Equilibration . . . . .	16
4.3	Autocorrelation times and error analysis . . . . .	17
4.4	Critical slowing down and the Wolff cluster algorithm . .	18
4.5	When does simple Monte Carlo fail? . . . . .	19
<b>5</b>	<b>Complex toy model: The Ising spin glass . . . . .</b>	<b>19</b>
5.1	Selected hallmark properties of spin glasses . . . . .	21
5.2	Theoretical description . . . . .	21
<b>6</b>	<b>Parallel tempering Monte Carlo . . . . .</b>	<b>22</b>
6.1	Outline of the algorithm . . . . .	23
6.2	Selecting the temperatures . . . . .	24
6.3	Example: Application to spin glasses . . . . .	25
<b>7</b>	<b>Rare events: Probing tails of energy distributions . . . . .</b>	<b>27</b>
7.1	Case study: Ground-state energy distributions . . . . .	27
7.2	Simple sampling . . . . .	27
7.3	Importance sampling with a guiding function . . . . .	28
7.4	Example: The Sherrington-Kirkpatrick Ising spin glass .	29
<b>8</b>	<b>Other Monte Carlo methods . . . . .</b>	<b>31</b>

---

## 1 Introduction

The Monte Carlo method in computational physics is possibly one of the most important numerical approaches to study problems spanning *all* thinkable scientific disciplines. The idea is seemingly simple: Randomly *sample* a volume in  $d$ -dimensional space to obtain an estimate of an *integral* at the price of a statistical error. For problems where the phase space dimension is very large—this is especially the case when the dimension of phase space depends on the number of degrees of freedom—the Monte Carlo method outperforms any other integration scheme. The difficulty lies in smartly choosing the random samples to minimize the numerical effort.

The term *Monte Carlo* method was coined in the 1940s by physicists S. Ulam, E. Fermi, J. von Neumann, and N. Metropolis (amongst others) working on the nuclear weapons project at Los Alamos National Laboratory. Because random numbers (similar to processes occurring in a casino, such as the Monte Carlo Casino in Monaco) are needed, it is believed that this is the source of the name. Monte Carlo methods were central to the simulations done at the Manhattan Project, yet mostly hampered by the slow computers of that era. This also spurred the development of fast random number generators, discussed in another lecture of this series.

In this lecture, focus is placed on the standard Metropolis algorithm to study problems in statistical physics, as well as a variation known as exchange or parallel tempering Monte Carlo that is very efficient when studying problems in statistical physics with complex energy landscapes (e.g., spin glasses, proteins, neural networks) [1]. In

general, continuous phase transitions are discussed. First-order phase transitions are, however, beyond the scope of these notes.

## 2 Monte Carlo integration

The motivation for Monte Carlo integration lies in the fact that most standard integration schemes fail for high-dimensional integrals. At the same time, the space dimension of the phase space of typical physical systems is very large. For example, the phase space dimension for  $N$  classical particles in three space dimensions is  $d = 6N$  (three coordinates and three momentum components are needed to fully characterize a particle). This is even worse for the case of  $N$  classical Ising spins (discussed below) which can take the values  $\pm 1$ . In this case the phase space dimension is  $2^N$ , a number that grows exponentially fast with the number of spins! Therefore, integration schemes such as Monte Carlo methods, where the error is independent of the space dimension, are needed.

### 2.1 Traditional integration schemes

Before introducing Monte Carlo integration, let us review standard integration schemes to highlight the advantages of random sampling methods. In general, the goal is to compute the following *one-dimensional* integral

$$I = \int_a^b f(x) dx . \quad (1)$$

Traditionally, one partitions the interval  $[a, b]$  into  $M$  slices of width  $\delta = (b - a)/M$  and then performs a  $k$ th order interpolation of the function  $f(x)$  for each interval to approximate the integral as a discrete sum (see Fig. 1). For example, to first order, one performs the *midpoint rule* where the area of the  $l$ th slice is approximated by a rectangle of width  $\delta$  and height  $f[(x_l + x_{l+1})/2]$ . It follows that

$$I \approx \sum_{l=0}^{M-1} \delta \cdot f[(x_l + x_{l+1})/2] . \quad (2)$$

For  $M \rightarrow \infty$  the discrete sum converges to the integral of  $f(x)$ . Convergence can be improved by replacing the rectangle with a linear interpolation between  $x_l$  and  $x_{l+1}$  (trapezoidal rule) or a weighted quadratic interpolation (Simpson's rule) [74]. One can show that the error made due to the approximation of the function is proportional to  $\sim M^{-1}$  for the midpoint rule if the function is evaluated at one of the interval's edges (in the center as shown above  $\sim M^{-2}$ ),  $\sim M^{-2}$  for the trapezoidal rule, and  $\sim M^{-4}$  for Simpson's rule. The convergence of the midpoint rule can thus be slow and the method should be avoided.

A problem arises when a multi-dimensional integral needs to be computed. In this case one can show that, for example, the error of Simpson's rule scales as  $\sim M^{-4/d}$

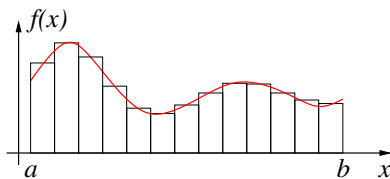


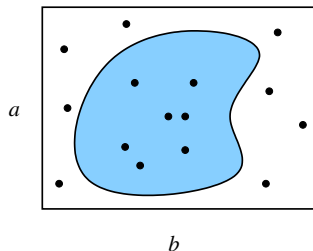
**Figure 1:** Illustration of the midpoint rule. The integration interval  $[a, b]$  is divided into  $M$  slices, the area of each slice approximated by the width of the slice,  $\delta = (b - a)/M$ , times the function evaluated at the midpoint of each slice.

because each space component has to be partitioned independently. Clearly, for space dimensions larger than 4 convergence becomes very slow. Similar arguments apply for any other traditional integration scheme where the error scales as  $\sim M^{-\kappa}$ : if applied to a  $d$ -dimensional integral the error scales  $\sim M^{-\kappa/d}$ .

## 2.2 Simple and Markov-chain sampling

One way to overcome the limitations imposed by high-dimensional volumes is *simple sampling* Monte Carlo. A simple analogy is to determine the area of a pond by throwing rocks. After enclosing the pond with a known area (e.g., a rectangle) and having enough beer or wine [2], pebbles are randomly thrown into the enclosed area. The ratio of stones in the pond and the total number of thrown stones is a *simple sampling* statistical estimate for the area of the pond, see Fig. 2.

**Figure 2:** Illustration of simple-sampling Monte Carlo integration. An unknown area (pond) is enclosed by a rectangle of known area  $A = ab$ . By randomly sampling the area with pebbles, a statistical estimate of the pond's area can be computed.



A slightly more “scientific” example is to compute  $\pi$  by applying Monte Carlo integration to the unit circle. The area of the unit circle is given by  $A_o = \pi r^2$  with  $r = 1$ ; the top right quadrant can be enclosed by a square of size  $r$  and area  $A_{\square} = r^2$  (see Fig. 3). An estimate of  $\pi$  can be accomplished with the following pseudo-code algorithm [3] that performs a simple sampling of the top-right quadrant:

```

1 algorithm simple_pi
2   initialize n_hits      0
3   initialize m_trials   10000
4   initialize counter    0
5
6   while(counter < m_trials) do

```

```

7     x = rand(0,1)
8     y = rand(0,1)
9     if(x**2 + y**2 < 1)
10        n_hits++
11    fi
12    counter++
13 done
14
15 return pi = 4*n_hits/m_trials

```

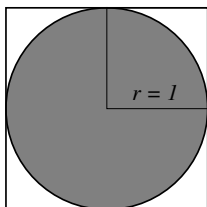


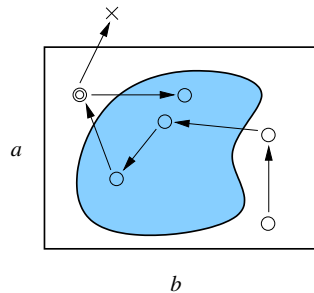
**Figure 3:** Monte Carlo estimate of  $\pi$  by randomly sampling the unit circle: two random numbers  $x$  and  $y$  in the range  $[0, 1]$  are computed. If  $x^2 + y^2 \leq 1$ , the resulting point is in the unit circle. After  $M$  trials an estimate of  $\pi/4$  can be computed with a statistical error  $\sim M^{-1/2}$ .

For each of the `m_trials` trials we generate two uniform random numbers [74] in the interval  $[0, 1]$  [with `rand(0,1)`] and test in line 9 of the algorithm if these lie in the unit circle or not. The counter `n_hits` is then updated if the resulting number is *in* the circle. In line 15 a statistical estimate of  $\pi$  is then returned.

Before applying these ideas to the integration of a function, we introduce the concept of a *Markov chain* [64]. In the simple-sampling approach to estimate the area of a pond as presented above, the random pebbles used are independent in the sense that a newly-selected pebble to be thrown into the rectangular area in Fig. 2 does not depend in any way on the position of the previous pebbles. If, however, the pond is very large, it is impossible to throw pebbles randomly from one position. Thus the approach is modified: After enough beer you start at a random location (make sure to drain the pond first) and throw a pebble into a random direction. You then walk to that pebble, pull a new pebble out of a pebble bucket you have with you and repeat the operation. This is illustrated in Fig. 4. If the pebble lands *outside* the rectangular area, the thrower should go get the outlier and place it on the *current* position of the thrower, i.e., if the move lies outside the sampled area, it is *rejected* and the last move counted twice. Why? This will be explained later and is called *detailed balance* (see p. 14). Basically, it ensures that the Markov chain is reversible. After many beers and throws, pebbles are scattered around the rectangular area, with small piles of multiple pebbles closer to the boundaries (due to rejected moves).

Again, these ideas can be used to estimate  $\pi$  by Markov-chain sampling the unit circle. Later, the Metropolis algorithm, which is based on these simple ideas, is introduced in detail using models from statistical physics. The following algorithm describes Markov-chain Monte Carlo for estimating  $\pi$ :

**Figure 4:** Illustration of Markov-chain Monte Carlo. The new state is always derived from the previous state. At each step a pebble is thrown in a random direction, the following throw has its origin at the landing position of the previous one. If a pebble lands outside the rectangular area (cross) the move is rejected and the last position recorded twice (double circle).



```

1 algorithm markov_pi
2   initialize n_hits      0
3   initialize m_trials   10000
4   initialize x          0
5   initialize y          0
6   initialize counter    0
7
8   while(counter < m_trials) do
9     dx = rand(-p,p)
10    dy = rand(-p,p)
11    if(|x + dx| < 1 and |y + dy| < 1)
12      x = x + dx
13      y = y + dy
14    fi
15    if(x**2 + y**2 < 1)
16      n_hits++
17    fi
18    counter++
19  done
20
21 return pi = 4*n_hits/m_trials
    
```

The algorithm starts from a given position in the space to be sampled [here  $(0, 0)$ ] and generates the position of the new dot from the position of the previous one. If the new position is outside the square, it is rejected (line 11). A careful selection of the step size  $p$  used to generate random numbers in the range  $[-p, p]$  is of importance: When  $p$  is too small, convergence is slow, whereas if  $p$  is too large many moves are rejected because the simulation will often leave the unit square. Therefore, a value of  $p$  has to be selected such that consecutive moves are accepted approximately 50% of the time.

The simple-sampling approach has the advantage over the Markov-chain approach in that the different samples are independent and thus not correlated. In the Markov-chain approach the new state depends on the previous state. This can be a problem since there might be a “memory” associated with this behavior. If this memory is large, then the *autocorrelation times* (i.e., the time it takes the system to forget where

it was) are large and many moves have to be discarded. Then why even think about the Markov-chain approach? Because in the study of physical systems it is generally easier to slightly (and randomly) change an existing state than to generate a new state from scratch for each step of the calculation. For example, when studying a system of  $N$  spins it is easier to flip one spin according to a given probability distribution than to generate a new configuration from scratch with a pre-determined probability distribution.

Let us apply now these ideas to perform a simple-sampling estimate of the integral of an actual function. As an example, we select a simple function, namely

$$f(x) = x^n \quad \rightarrow \quad I = \int_0^1 f(x) dx \quad (3)$$

with  $n > -1$ . Using simple-sampling Monte Carlo, the integral can be estimated via

```

1 algorithm simple_integrate
2   initialize integral  0
3   initialize m_trials  10000
4   initialize counter   0
5
6   while(counter < m_trials) do
7     x = rand(0,1)
8     integral += x**n
9     counter++
10  done
11
12 return integral/m_trials
```

In line 8 we evaluate the function at the random location and add the result to the estimate of the integral, i.e.,

$$I \approx \frac{1}{M} \sum_i^M f(x_i), \quad (4)$$

where we have set `m_trials` =  $M$ . To calculate the error of the estimate, we need to compute the variance of the function. For this we need to also perform a simple sampling of the square of the function, i.e., add a line to the code with `integral_square += x**(2*n)`. It then follows [56] for the statistical error of the integral  $\delta I$

$$\delta I = \sqrt{\frac{\text{Var} f}{M-1}}, \quad \text{Var} f = \langle f^2 \rangle - \langle f \rangle^2, \quad (5)$$

with

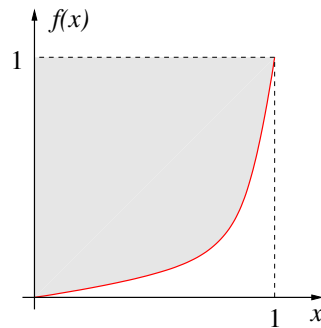
$$\langle f^k \rangle = \int_0^1 [f(x)]^k dx \approx \frac{1}{M} \sum_i^M [f(x_i)]^k. \quad (6)$$

Here  $x_i$  are uniformly distributed random numbers. The important detail is that Eq. (5) does *not* depend on the space dimension and merely on  $M^{-1/2}$ . This means

that, for example, for space dimensions  $d > 8$  Monte Carlo sampling outperforms Simpson's rule.

The presented simple-sampling approach has one crucial problem: When in the example shown the exponent  $n$  is close to  $-1$  or much larger than  $1$  the variance of the function in the interval is large. At the same time, the interval  $[0, 1]$  is sampled uniformly. Therefore, similar to the estimate of  $\pi$ , areas which carry little weight for the integral are sampled with equal probability as areas which carry most of the function's support (see Fig. 5). Therefore the integral and error converge slowly. To alleviate the situation and shift resources where they are needed most, *importance sampling* is used.

**Figure 5:** Illustration of the simple-sampling approach when integrating  $f(x) = x^n$  with  $n \gg 1$ . The function has most support for  $x \rightarrow 1$ . Because random numbers are generated with a uniform probability, the whole range  $[0, 1]$  is sampled equally probable, although for  $x \rightarrow 0$  the contribution to the integral is small. Thus, the integral converges slowly.



## 2.3 Importance sampling

When the variance of the function to be integrated is large, the error [directly dependent on the variance, see Eq. (5)] is also large. A cure to the problem is provided by generating random numbers that more efficiently sample the area, i.e., distributed according to a function  $p(x)$  which, if possible, has to fulfill the following criteria: First,  $p(x)$  should be as close as possible to  $f(x)$  and second, generating  $p$ -distributed random numbers should be easily accomplished. The integral of  $f(x)$  can be expressed in the following way [using the notation introduced in Eq. (6)]

$$\langle f \rangle = \langle f/p \rangle_p = \int_0^1 \frac{f(x)}{p(x)} p(x) dx \approx \frac{1}{M} \sum_i^M \frac{f(y_i)}{p(y_i)}. \quad (7)$$

In Eq. (7)  $\langle \dots \rangle_p$  corresponds to a sampling with respect to  $p$ -distributed random numbers;  $y_i$  are also  $p$ -distributed. The advantage of this approach is that the error is now given in terms of the variance  $\text{Var}(f/p)$  and, if both  $f(x)$  and  $p(x)$  are close, the variance of  $f/p$  is considerably smaller than the variance of  $f$ .

For the case of  $f(x) = x^n$  we could, for example, select random numbers distributed according to  $p(x) \sim x^\ell$  with  $\ell \geq n$  (when  $n > -1$ ). This means that in Fig. 5 the area around  $x \lesssim 1$  is sampled with a higher probability than the area



around  $x \sim 0$ . Power-law distributed random numbers  $y$  can be readily produced from uniform random numbers  $x$  by inverting the cumulative distribution of  $p(x)$ , i.e.,

$$y(x) = x^{1/(\ell+1)}, \quad \ell > -1. \quad (8)$$

In the next sections the elaborated concepts are applied to problems in (statistical) physics. First, some toy models and physical approaches to study the critical behavior of statistical models using finite-size simulations are introduced.

### 3 Interlude: Statistical mechanics

In this section the core concepts of statistical mechanics are presented as well as a simple model to study phase transitions. Because discussing these topics at length is beyond the scope of these lecture notes, the reader is referred to the vast literature in statistical physics, in particular Refs. [18, 31, 36, 43, 77, 79, 91].

#### 3.1 Simple toy model: The Ising model

Developed in 1925 [45] by Ernst Ising and Wilhelm Lenz, the Ising model has become over the decades the drosophila of statistical mechanics. The simplicity yet rich behavior of the model makes it the perfect platform to study many magnetic systems as well as for testing of algorithms. For simplicity, it is assumed that the magnetic moments are highly anisotropic, i.e., they can only point in one space direction. The classical spins  $S_i = \pm 1$  are placed on a hypercubic lattice with nearest-neighbor interactions. Therefore, the Hamiltonian is given by

$$\mathcal{H} = \sum_{\langle i,j \rangle} J_{ij} S_i S_j - H \sum_i S_i. \quad (9)$$

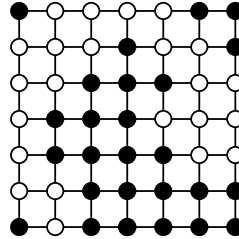
The first term in Eq. (9) is responsible for the pairwise interaction between two neighboring spins  $S_i$  and  $S_j$ . When  $J_{ij} = -J < 0$ , the energy is minimized by aligning all spins, i.e., ferromagnetic order, whereas when  $J_{ij} = J > 0$  the energy is minimized by ensuring that the product over all neighboring spins is negative. In this case, staggered antiferromagnetic order is obtained for  $T \rightarrow 0$ . The “ $\langle i, j \rangle$ ” represents a sum over nearest-neighbor pairs of spins on the lattice (see Fig. 6). The second term in Eq. (9) represents a coupling to an external field of strength  $H$ . Amazingly, this simple model captures all interesting phenomena found in the physics of statistical mechanics and phase transitions. It is exactly solvable in one space dimension, and in two dimensions for  $H = 0$ , and thus an excellent test bed for algorithms. Furthermore, in space dimensions larger than one it undergoes a finite-temperature transition into an ordered state.

A natural way to quantify the temperature-dependent transition in the ferromagnetic case is to measure the magnetization

$$m = \frac{1}{N} \sum_i S_i \quad (10)$$

of the system. When all spins are aligned, i.e., at low temperatures (below the transition), the magnetization is close to unity. For temperatures much larger than the transition temperature  $T_c$ , spins fluctuate wildly and so, on average, the magnetization is zero. Therefore, the magnetization plays the role of an *order parameter* that is large in the ordered phase and zero otherwise. Before the model is described further, some basic concepts from statistical physics are introduced.

**Figure 6:** Illustration of the two-dimensional Ising model with nearest-neighbor interactions. Filled [open] circles represent  $S_i = +1$  [ $S_i = -1$ ]. The spins only interact with their nearest neighbors (lines connecting the dots).



### 3.2 Statistical physics in a nutshell

It would be beyond the scope of this lecture to discuss in detail statistical mechanics of magnetic systems. The reader is referred to the vast literature on the topic [18, 31, 36, 43, 77, 79, 91]. In this context only the relevant aspects of statistical physics are discussed.

**Observables** In statistical physics, expectation values of quantities such as the energy, magnetization, specific heat, etc.—generally called *observables*—are computed by performing a trace over the partition function  $\mathcal{Z}$ . Within the *canonical ensemble* [43] where the temperature  $T$  is fixed, the *expectation value* or thermal average of an observable  $\mathcal{O}$  is given by

$$\langle \mathcal{O} \rangle = \frac{1}{\mathcal{Z}} \sum_s \mathcal{O}(s) e^{-\mathcal{H}(s)/kT} . \quad (11)$$

The sum is over all states  $s$  in the system, and  $k$  represents the Boltzmann constant.  $\mathcal{Z} = \sum_s \exp[-\mathcal{H}(s)/kT]$  is the partition function which normalizes the equilibrium Boltzmann distribution

$$\mathcal{P}_{\text{eq}}(s) = \frac{1}{\mathcal{Z}} e^{-\mathcal{H}(s)/kT} . \quad (12)$$

The  $\langle \dots \rangle$  in Eq. (11) represent a thermal average. One can show that the internal energy of the system is given by

$$E = \langle \mathcal{H}(s) \rangle , \quad (13)$$

whereas the free energy  $\mathcal{F}$  is given by

$$\mathcal{F} = -kT \ln \mathcal{Z} . \quad (14)$$

Note that *all* thermodynamic quantities can be computed directly from the partition function and expressed as derivatives of the free energy (see Ref. [91] for details). Because the partition function is closely related to the Boltzmann distribution, it follows that if we can *sample* observables (e.g., measure the magnetization) with states generated according to the corresponding Boltzmann distribution, a simple Markov-chain “integration” scheme can be used to produce an estimate.

**Phase transitions** Continuous phase transitions [43] have no latent heat at the transition and are thus easier to describe. At a continuous phase transition the free energy has a singularity that usually manifests itself via a power-law behavior of the derived observables at criticality. The correlation length  $\xi$  [43]—which gives us a measure of correlations and order in a system—diverges at the transition

$$\xi \sim |T - T_c|^{-\nu}, \quad (15)$$

with  $\nu$  a critical exponent quantifying this divergence and  $T_c$  the transition temperature. Close enough to the transition (i.e.,  $|T - T_c|/T_c \ll 1$ ) the behavior of observables can be well described by power laws. For example, the specific heat  $c_V$  has a singularity at  $T_c$  with  $c_V \sim |T - T_c|^{-\alpha}$ , although the exponent  $\alpha$  (unlike  $\nu$ ) can be both negative and positive. The magnetization does not diverge, but has a singular kink at  $T_c$ , i.e.,  $m \sim |T - T_c|^\beta$  with  $\beta > 0$ .

Using arguments from the renormalization group [31] it can be shown that the critical exponents are related via *scaling* relations. Often (as in the Ising case), only two exponents are independent and *fully* characterize the critical behavior of the model. It can be further shown that models in statistical physics generally obey *universal behavior* (there are some exceptions. . .), i.e., if the lattice geometry is kept the same, the critical exponents *only* depend on the order parameter symmetry. Therefore, when simulating a statistical model, it is enough to determine the location of the transition temperature  $T_c$ , as well as *two independent* critical exponents to fully characterize the *universality class* of the system.

**Finite-size scaling and the Binder ratio (or “Binder cumulant”)** How can we determine the *bulk* critical exponents of a system by simulating finite lattices? When the systems are not infinitely large, the critical behavior is smeared out. Again, using arguments from the renormalization group, one can show that the nonanalytic part of a given observable can be described by a *finite-size scaling* form [75]. For example, the finite-size magnetization from a simulation of an Ising system with  $L^d$  spins is asymptotically (close to the transition, and for large  $L$ ) given by

$$\langle m_L \rangle \sim L^{\beta/\nu} \tilde{M}[L^{1/\nu}(T - T_c)], \quad (16)$$

and for the magnetic susceptibility by

$$\chi_L \sim L^{\gamma/\nu} \tilde{C}[L^{1/\nu}(T - T_c)], \quad (17)$$

where close to the transition  $\chi \sim |T - T_c|^{-\gamma}$  (for the infinite system,  $L \rightarrow \infty$ ) and

$$\chi = \frac{L^d}{kT} (\langle m^2 \rangle - \langle m \rangle^2) . \quad (18)$$

Both  $\tilde{M}$  and  $\tilde{C}$  are unknown *scaling functions*. Equations (16) and (17) show that when  $T = T_c$ , data for  $\langle m_L \rangle / L^{\beta/\nu}$  and  $\chi_L / L^{\gamma/\nu}$  simulated for different system sizes  $L$  should cross in the large- $L$  limit at one point, namely  $T = T_c$ , provided we use the right expressions for  $\beta/\nu$  and  $\gamma/\nu$ , respectively. In reality, there are nonanalytic corrections to scaling and so the crossing points between two *successive* system size pairs (e.g.,  $L$  and  $2L$ ) converge to a common crossing point for  $L \rightarrow \infty$  that agrees with the bulk transition temperature  $T_c$ . Performing the finite-size scaling analysis with the magnetization or the susceptibility is not very practical, because neither  $\beta$  nor  $\gamma$  are known a priori. There are other approaches to determine these, but a far simpler method is to determine *combined* quantities that are dimensionless. One such quantity is known as the *Binder ratio* (or “Binder cumulant”) [12] given by

$$g = \frac{1}{2} \left[ 3 - \frac{\langle m^4 \rangle}{\langle m^2 \rangle^2} \right] \sim \tilde{G}[L^{1/\nu}(T - T_c)] . \quad (19)$$

The different factors ensure that  $g \rightarrow 1$  for  $T \rightarrow 0$  and  $g \rightarrow 0$  for  $T \rightarrow \infty$ . The asymptotic (for large  $L$ ) scaling behavior of the Binder ratio follows directly from the fact that the pre-factors of the moments of the magnetization ( $m^k \sim L^{k\beta/\nu}$ ) cancel out in Eq. (19).

The Binder ratio is a *dimensionless* quantity and so data for different system sizes  $L$  approximately cross at a putative transition—provided corrections to scaling are small. Furthermore, by carefully selecting the correct value of the critical exponent  $\nu$ , the data fall onto a universal curve. Therefore, the method allows for an estimation of  $T_c$ , as well as the critical exponent  $\nu$ . This is illustrated in Fig. 7 for the two-dimensional Ising model. The left panel shows the Binder ratio as a function of temperature for several small system sizes. The vertical dashed line marks the exactly-known value of the critical temperature, namely  $T_c = 2/\ln(1 + \sqrt{2}) \approx 2.269\dots$  [91]. The right panel shows a finite-size scaling analysis of the data for the exact value of the critical exponent  $\nu$ . Close to the transition the data fall onto a universal curve, showing that  $\nu = 1$  is the correct value of the critical exponent. The two-dimensional Ising universality class is fully characterized with a second critical exponent, e.g.,  $\beta = 1/8$ .

Note that other dimensionless quantities, such as the two-point finite-size correlation length [7, 70] can also be used with similar results.

## 4 Monte Carlo simulations in statistical physics

In analogy to the importance-sampling Monte Carlo integration of functions discussed in Sec. 2, we can use the gained insights to sample the average of an observable in

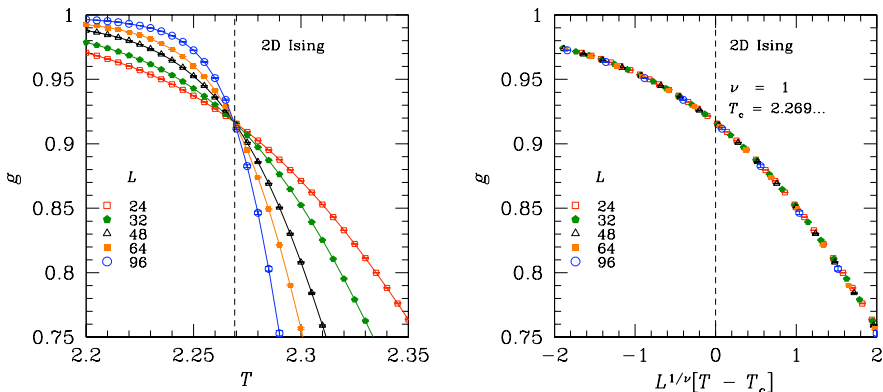


**Figure 7:** Left panel: Binder ratio as a function of temperature for the two-dimensional Ising model with nearest-neighbor interactions. The data approximately cross at one point (the dashed line corresponds to the exactly-known  $T_c$  for the two-dimensional Ising model) signaling a transition. Right panel: Finite-size scaling of the data in the left panel using the known  $T_c = 2.269\dots$  and  $\nu = 1$ . Plotted are data for the Binder ratio as a function of the scaling variable  $L^{1/\nu}[T - T_c]$ . Data for different system sizes fall onto a universal curve suggesting that the parameters used are the correct ones.

statistical physics. In general, as shown in Eq. (11),

$$\langle \mathcal{O} \rangle = \frac{\sum_s \mathcal{O}(s) e^{-\mathcal{H}(s)/kT}}{\sum_s e^{-\mathcal{H}(s)/kT}}. \quad (20)$$

Equation (20) can be trivially extended with a distribution for the states, i.e.,

$$\langle \mathcal{O} \rangle = \frac{\sum_s [\mathcal{O}(s) e^{-\mathcal{H}(s)/kT} / \mathcal{P}(s)] \mathcal{P}(s)}{\sum_s [e^{-\mathcal{H}(s)/kT} / \mathcal{P}(s)] \mathcal{P}(s)}. \quad (21)$$

The approach is completely analogous to the importance sampling Monte Carlo integration. If  $\mathcal{P}(s)$  is the Boltzmann distribution [Eq. (12)] then the factors cancel out and we obtain

$$\langle \mathcal{O} \rangle = \frac{1}{M} \sum_i \mathcal{O}(s_i), \quad (22)$$

where the states  $s_i$  are now selected according to the Boltzmann distribution. The problem now is to find an algorithm that allows for a sampling of the Boltzmann distribution. The method is known as the Metropolis algorithm.

## 4.1 Metropolis algorithm

The Metropolis algorithm [63] was developed in 1953 at Los Alamos National Lab within the nuclear weapons program mainly by the Rosenbluth and Teller families [4]. The article in the Journal of Chemical Physics starts in the following way:

*“The purpose of this paper is to describe a general method, suitable for fast electronic computing machines, of calculating the properties of any substance which may be considered as composed of interacting individual molecules.”*

And they were right. The idea is the following: In order to evaluate Eq. (20) we generate a Markov chain of successive states  $s_1 \rightarrow s_2 \rightarrow \dots$ . The new state is generated from the old state with a carefully-designed transition probability  $\mathcal{P}(s \rightarrow s')$  such that it occurs with a probability given by the equilibrium Boltzmann distribution, i.e.,  $\mathcal{P}_{\text{eq}}(s) = Z^{-1} \exp[-\mathcal{H}(s)/kT]$ . In the Markov process, the state  $s$  occurs with probability  $\mathcal{P}_k(s)$  at the  $k$ th time step, described by the master equation

$$\mathcal{P}_{k+1}(s) = \mathcal{P}_k(s) + \sum_{s'} [\mathcal{T}(s' \rightarrow s)\mathcal{P}_k(s') - \mathcal{T}(s \rightarrow s')\mathcal{P}_k(s)] . \quad (23)$$

The sum is over all states  $s'$  and the first term in the sum describes all processes *reaching* state  $s$ , while the second term describes all processes *leaving* state  $s$ . The goal is that for  $k \rightarrow \infty$  the probabilities  $\mathcal{P}_k(s)$  reach a stationary distribution described by the Boltzmann distribution. The transition probabilities  $\mathcal{T}$  can be designed in such a way that for  $\mathcal{P}_k(s) = \mathcal{P}_{\text{eq}}(s)$ , all terms in the sum vanish, i.e., for all  $s$  and  $s'$  the *detailed balance* condition

$$\mathcal{T}(s' \rightarrow s)\mathcal{P}_{\text{eq}}(s') = \mathcal{T}(s \rightarrow s')\mathcal{P}_{\text{eq}}(s) \quad (24)$$

must hold. The condition in Eq. (24) means that the process has to be reversible. Furthermore, when the system has assumed the equilibrium probabilities, the ratio of the transition probabilities only depends on the change in energy  $\Delta\mathcal{H}(s, s') = \mathcal{H}(s') - \mathcal{H}(s)$ , i.e.,

$$\frac{\mathcal{T}(s \rightarrow s')}{\mathcal{T}(s' \rightarrow s)} = \exp[-(\mathcal{H}(s') - \mathcal{H}(s))/kT] = \exp[-\Delta\mathcal{H}(s, s')/kT] . \quad (25)$$

There are different choices for the transition probabilities  $\mathcal{T}$  that satisfy Eq. (25). One can show that  $\mathcal{T}$  has to satisfy the general equation  $\mathcal{T}(x)/\mathcal{T}(1/x) = x \forall x$  with  $x = \exp(-\Delta\mathcal{H}/kT)$ . There are two convenient choices for  $\mathcal{T}$  that satisfy this condition:

**1. Metropolis (also known as Metropolis-Hastings) algorithm** In this case  $\mathcal{T}(x) = \min(1, x)$  and so

$$\mathcal{T}(s \rightarrow s') = \begin{cases} \Gamma, & \text{if } \Delta\mathcal{H} \leq 0; \\ \Gamma e^{-\Delta\mathcal{H}(s, s')/kT}, & \text{if } \Delta\mathcal{H} \geq 0. \end{cases} \quad (26)$$

In Eq. (26),  $\Gamma^{-1}$  represents a Monte Carlo time.

**2. Heat-bath algorithm** In this case  $\mathcal{T}(x) = x/(1+x)$  corresponding to an acceptance probability  $\sim [1 + \exp(\Delta\mathcal{H}(s, s')/kT)]^{-1}$ . For the rest of this lecture, we

focus on the Metropolis algorithm. The heat bath algorithm is more efficient when temperatures far below the transition temperature are sampled.

The move between states  $s$  and  $s'$  can, in principle, be arbitrary. If, however, the energies of states  $s$  and  $s'$  are too far apart, the move will likely not be accepted. For the case of the Ising model, in general, a single spin  $S_i$  is selected and flipped with the following probability:

$$\mathcal{T}(S_i \rightarrow -S_i) = \begin{cases} \Gamma, & \text{for } S_i = -\text{sign}(h_i); \\ \Gamma e^{-2S_i h_i/kT}, & \text{for } S_i = \text{sign}(h_i). \end{cases} \quad (27)$$

where  $h_i = -\sum_{j \neq i} J_{ij} S_j + H$  is the effective local field felt by the spin  $S_i$ .

**Practical implementation of the Metropolis algorithm** A simple pseudo-code Monte Carlo program to compute an observable  $\mathcal{O}$  for the Ising model is the following:

```
1 algorithm ising_metropolis(T,steps)
2   initialize starting configuration S
3   initialize  $\mathcal{O} = 0$ 
4
5   for(counter = 1 ... steps) do
6     generate trial state S'
7     compute  $p(S \rightarrow S', T)$ 
8      $x = \text{rand}(0,1)$ 
9     if( $p > x$ ) then
10      accept S'
11    fi
12
13     $\mathcal{O} += \mathcal{O}(S')$ 
14  done
15
16 return  $\mathcal{O}/\text{steps}$ 
```

After initialization, in line 6 a proposed state is generated by, e.g., flipping a spin. The energy of the new state is computed and henceforth the transition probability between states  $p = \mathcal{T}(S \rightarrow S')$ . A uniform random number  $x \in [0, 1]$  is generated. If the probability is larger than the random number, the move is accepted. If the energy is lowered, i.e.,  $\Delta\mathcal{H} > 0$ , the spin is always flipped. Otherwise the spin is flipped with a probability  $p$ . Once the new state is accepted, we measure a given observable and record its value to perform the thermal average at a given temperature. For  $\text{steps} \rightarrow \infty$  the average of the observable converges to the exact value, again with an error inversely proportional to the square root of the number of steps. This is the core bare-bones routine for the Metropolis algorithm. In practice, several aspects have to be considered to ensure that the data produced are correct. The most important, autocorrelation and equilibration times, are described below.

## 4.2 Equilibration

In order to obtain a correct estimate of an observable  $\mathcal{O}$ , it is imperative to ensure that one is actually sampling an *equilibrium* state. Because, in general, the initial configuration of the simulation can be chosen at random—popular choices being random or polarized configuration—the system will have to evolve for several Monte Carlo steps before an equilibrium state at a given temperature is obtained. The time  $\tau_{\text{eq}}$  until the system is in thermal equilibrium is called *equilibration time* and depends directly on the system size (e.g., the number of spins  $N = L^d$ ) and increases with decreasing temperature. In general, it is measured in units of *Monte Carlo sweeps* (MCS), i.e., 1 MCS =  $N$  spin updates.

In practice, all measured observables should be monitored as a function of MCS to ensure that the system is in thermal equilibrium. Some observables, such as the



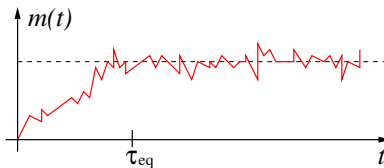


**Figure 8:** Sketch of the equilibration behavior of the magnetization  $m$  as a function of Monte Carlo time. After a certain time  $\tau_{\text{eq}}$  the data become approximately flat and fluctuate around a mean value. Once  $\tau_{\text{eq}}$  has been reached, the system is in thermal equilibrium and observables can be measured.

energy, equilibrate faster than others (e.g., magnetization) and thus the equilibration times of *all* observables measured need to be considered.

### 4.3 Autocorrelation times and error analysis

Because in a Markov chain the new states are generated by modifying the previous ones, subsequent states can be highly correlated. To ensure that the measurement of an observable  $\mathcal{O}$  is not biased by correlated configurations, it is important to measure the autocorrelation time  $\tau_{\text{auto}}$  that describes the time it takes for two measurements to be decorrelated. This means that in a Monte Carlo simulation, after the system has been thermally equilibrated, measurements can only be taken every  $\tau_{\text{auto}}$  MCS. To compute the autocorrelation time for a given observable  $\mathcal{O}$ , the time-dependent *autocorrelation* function needs to be measured:

$$C_{\mathcal{O}}(t) = \frac{\langle \mathcal{O}(t_0)\mathcal{O}(t_0+t) \rangle - \langle \mathcal{O}(t_0) \rangle \langle \mathcal{O}(t_0+t) \rangle}{\langle \mathcal{O}^2(t_0) \rangle - \langle \mathcal{O}(t_0) \rangle^2}. \quad (28)$$

In general,  $C_{\mathcal{O}}(t) \sim \exp(-t/\tau_{\text{auto}})$  and so  $\tau_{\text{auto}}$  is given by the value where  $C_{\mathcal{O}}$  drops to  $1/e$ . An alternative is the integrated autocorrelation time  $\tau_{\text{auto}}^{\text{int}}$ . It is basically the same as the standard autocorrelation time for any practical purpose. However, it is easier to compute:

$$\tau_{\text{auto}}^{\text{int}} = \frac{\sum_{t=1}^{\infty} (\langle \mathcal{O}(t_0)\mathcal{O}(t_0+t) \rangle - \langle \mathcal{O} \rangle^2)}{\langle \mathcal{O}^2 \rangle - \langle \mathcal{O} \rangle^2} \quad (29)$$

Autocorrelation effects influence the determination of the error of statistical estimates. It can be shown [36] that the error  $\Delta\mathcal{O}$  is given by

$$\Delta\mathcal{O} = \sqrt{\frac{\langle \mathcal{O}^2 \rangle - \langle \mathcal{O} \rangle^2}{(M-1)} (1 + 2\tau_{\text{auto}})}. \quad (30)$$

Here  $M$  is the number of measurements. The autocorrelation time directly influences the calculation of the error bars and must be computed and included in all calculations. So far, we have not discussed how the autocorrelation times depend on the system size and the temperature. Like the equilibration times, the autocorrelation times increase with increasing system size.

## 4.4 Critical slowing down and the Wolff cluster algorithm

Close to a phase transition, the autocorrelation time is given by

$$\tau_{\text{auto}} \sim \xi^z \quad (31)$$

with  $z > 1$  and typically around 2. Because the correlation length  $\xi$  diverges at a continuous phase transition, so does the autocorrelation time. This effect, known as *critical slowing down*, slows simulations to intractable times close to continuous phase transitions when the *dynamical critical exponent*  $z$  is large.

The problem can be alleviated by using Monte Carlo methods which, while only performing small changes to the energy of the system (to ensure that moves are accepted frequently), heavily randomize the spin configurations and not only change the value of one spin. This ensures that phase space is sampled evenly. Typical examples are *cluster algorithms* [82, 90] where a carefully-built cluster of spins is flipped at each step of the simulation [36, 58, 59, 68].

**Wolff cluster algorithm (Ising spins)** In the Wolff cluster algorithm [90] we choose a random spin and build a cluster around it (the algorithm is constructed in such a way that larger clusters are preferred). Once the cluster is constructed, it is flipped in a rejection-free move. This “randomizes” the system efficiently, thus overcoming critical slowing down. Outline of the algorithm:

- Select a random spin.
- If a neighboring spin is parallel to the initial spin, add it to the cluster with a probability  $1 - \exp(-2J/kT)$ .
- Repeat the previous step for all neighbors of the newly-added spins and iterate until no new spins can be added.
- Flip all spins in the cluster.

The algorithm obeys detailed balance. Furthermore, one can show that the linear size of the cluster is proportional to the correlation length. Therefore the algorithm adapts to the behavior of the system at criticality resulting in  $z \approx 0$ , i.e., the critical slowing down encountered around the transition is removed and the algorithm performs orders of magnitude faster than simple Monte Carlo. For low temperatures, the cluster algorithm merely “flip-flops” almost all spins of the system and provides not much improvement, unless a domain wall is stuck in the system. For temperatures much higher than the critical temperature the size of the clusters is of the order of one spin and there the Metropolis algorithm outperforms the cluster algorithm (keep in mind that building the cluster takes many operations). Thus the method works best at criticality.

In general, to be able to cover a temperature range that extends beyond the critical region, combinations of cluster updates and local updated (standard Monte Carlo) are recommended. One can also define *improved estimators* to measure observables with

a reduced statistical error. Finally, the Wolff cluster algorithm can also be generalized to Potts spins, XY and Heisenberg spins, as well as hard disks. The reader is referred to the literature [36, 56, 58, 59, 68] for details.

Note that the Swendsen-Wang cluster algorithm [82] is similar to the Wolff cluster algorithm. However, instead of building one cluster, multiple clusters are built. This is less efficient when the space dimension is larger than two because in that case only few large clusters will exist.

#### 4.5 When does simple Monte Carlo fail?

Metropolis *et al.* did not bear in mind that there are systems where even a simple spin flip can produce a huge change in the energy  $\Delta\mathcal{H}$  of the system. This has the effect that the probability for new configurations to be accepted is very small and the simulation stalls, in particular when the studied system has a rough energy landscape, i.e., different states in phase space are separated by large energy “mountains” and deep energy “valleys,” as depicted in Fig. 9. Examples of such complex systems are spin glasses, proteins and neural networks.

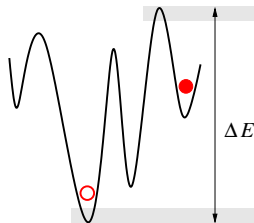


**Figure 9:** Sketch of a rough energy landscape. A Monte Carlo move from the initial (solid circle) to the final state (open circle) is unlikely if the size of the barrier  $\Delta E$  is large, especially at low temperatures. A simple Monte Carlo simulation will stall and the system will be stuck in the metastable state.

These systems are characterized by a complex energy landscape with deep valleys and mountains that grow exponentially with the system size. Therefore, for low temperatures, equilibration times of simple Monte Carlo methods diverge. Although the method technically still works, the time it takes to equilibrate even the smallest systems becomes impractical. Improved sampling techniques for rough energy landscapes need to be implemented.

## 5 Complex toy model: The Ising spin glass

What happens if we take the ferromagnetic Ising model and flip the sign of randomly-selected interactions  $J_{ij}$  between two spins? The resulting behavior is illustrated in Fig. 10. For low temperatures, if the product of the interactions  $J_{ij}$  around any plaquette is negative, *frustration* effects emerge. The spin in the lower left corner of the highlighted plaquette tries to minimize the energy by either aligning with the right neighbor, or being antiparallel with the top neighbor. Both conditions are mutually exclusive and so the energy cannot be uniquely minimized. This behavior

is a hallmark of spin glasses [13, 21, 23, 28, 65, 83, 92]. Note that, in general, the bonds are either chosen from a bimodal ( $\mathcal{P}_b$ ) or Gaussian ( $\mathcal{P}_g$ ) disorder distribution:

$$\mathcal{P}_b(J_{ij}) = p\delta(J_{ij} - 1) + (1 - p)\delta(J_{ij} + 1), \quad \mathcal{P}_g(J_{ij}) = \frac{1}{\sqrt{2\pi}} \exp[-J_{ij}^2/2], \quad (32)$$

where, in general  $p = 1/2$ . The Hamiltonian in Eq. (9) with disorder in the bonds is known as the Edwards-Anderson Ising spin glass. There is a finite-temperature transition for space dimensions  $d \geq 3$  between a spin-glass and the (thermally) disordered state, cf. Sec. 5.2. For example, for Gaussian disorder in three space dimensions  $T_c \approx 0.95$  [49].

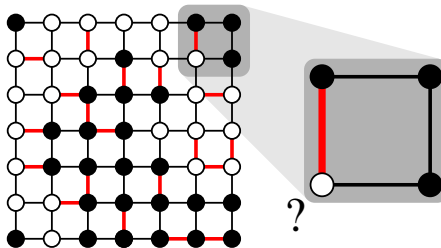


**Figure 10:** Two-dimensional Ising spin-glass. The circles represent Ising spins. A thin line between two spins  $i$  and  $j$  corresponds to  $J_{ij} < 0$ , whereas a thick line corresponds to  $J_{ij} > 0$ . In comparison to a ferromagnet, the behavior of the model system changes drastically, as illustrated in the highlighted plaquette. For  $T \rightarrow 0$ , the spin in the lower left corner is unable to fulfill the interactions with the neighbors and is *frustrated* (see text).

The result of competing interactions is a complex energy landscape. The complexity of the model increases considerably. For example, finding the ground state energy of a spin glass is generally an NP-hard problem. Equilibration times in finite-temperature Monte Carlo simulations grow exponentially and thus the study of system sizes beyond a few spins becomes intractable. So ... why study these systems? Not only are there many materials [13] that can be described well with spin-glass Hamiltonians, many other problems spanning several fields of science can be either described directly by spin-glass Hamiltonians or mapped onto these. Therefore these models are of general interest to a broad spectrum of disciplines.

Note that, because in general only finite system sizes can be simulated, an average over different realizations of the disorder needs to be performed in addition to the thermal averages. This means that after a Monte Carlo simulation has been completed for a given distribution of the disorder, it must be repeated at least 1000 times for the results to be representative. Although this extra effort further complicates simulations of spin-glass systems, it makes them *embarrassingly* parallel, i.e., simulations can easily be distributed over many workstations.

## 5.1 Selected hallmark properties of spin glasses

Because of the complex energy landscape, spin glasses show dynamical properties not seen in any other materials/systems. First, spin-glass observables such as susceptibilities and magnetizations *age* with time. Due to the complex energy landscape, there are rearrangements of the spins in macroscopic time scales. Therefore, when preparing a spin-glass system at a given temperature, a slow decay of observables can be observed because the system, at least experimentally, is never in thermal equilibrium. Furthermore, when performing an aging experiment on a spin glass, changing the temperature from  $T_1 < T_c$  to  $T_2 < T_1$  at time  $t_1$  for a finite period of time  $t_2$  and then back to  $T_1$  shows interesting *memory* effects [47]. After the time  $t_1 + t_2$ , the system remembers the state it had at time  $t_1$  and follows the previous aging path. This memory and rejuvenation effect is unique to spin glasses.

While the susceptibility shows a cusp at the transition [17], the specific heat has a smooth behavior around the transition temperature [65]. Furthermore, no signs of spatial ordering can be found when performing a neutron scattering experiment probing below the transition temperature. However, Mössbauer spectroscopy shows that the magnetic moments are frozen in space, thus indicating that the system is in a glassy and not liquid phase. Therefore, in its simplest interpretation, a spin glass is a model for a highly-disordered magnet.

## 5.2 Theoretical description

In 1975, Edwards and Anderson suggested a phenomenological model in order to describe these fascinating materials: the Edwards-Anderson (EA) spin-glass Hamiltonian [25] discussed above. In 1979, Parisi postulated a solution (only recently proven to be correct [84]) to the mean-field Sherrington-Kirkpatrick (SK) model [78], a variation of the Edwards-Anderson model with *infinite-range interactions* (all spins interact with each other). The replica symmetry breaking picture (RSB) of Parisi for the mean-field model spawned an increased interest in the field and has been applied to a variety of problems. In addition, in 1986 a phenomenological description, called the “Droplet Picture” (DP) was introduced simultaneously by Fisher & Huse and Bray & Moore [26, 27] in order to describe short-range spin glasses, as well as the chaotic pairs picture by Newman & Stein [66, 67]. However, rigorous analytical results are difficult to obtain for realistic short-range spin-glass models. Because of this, research has shifted to intense *numerical studies*.

Nevertheless, spin glasses are far from being understood. The memory effect in spin glasses [47] has yet to be understood theoretically, and only recently was it observed numerically [46]. The existence of a spin-glass phase in a finite magnetic field [20] has been a source of debate [93], as well as the ultrametric structure of the phase space (hierarchical structure of states) which remains to be understood for realistic models [39, 48]. Finally, there have been several numerical attempts at finite [42, 50, 57, 62, 71] and zero temperature [34, 38] to better understand the nature of the spin-glass state for short-range spin glasses. To date, the data for Ising spins are consistent with an intermediate picture [57, 71] that combines elements from the

standard theoretical predictions of replica symmetry breaking and the droplet theory.

How can order be quantified in a system that intrinsically does not have visible spatial order? For this we need to first determine what differentiates a spin glass at temperatures above the critical point  $T_c$  and below. Above the transition, like for the regular Ising model, spins fluctuate and any given snapshot yields a random configuration. Therefore, comparing a snapshot at time  $t$  and time  $t + \delta t$  yields completely different results. Below the transition, (replica) symmetry is broken and configurations freeze into place. Therefore, comparing a snapshot of the system at time  $t$  and time  $t + \delta t$  shows significant similarities. A natural choice thus is to define an *overlap* function  $q$  which compares two copies of the system with the *same* disorder.

In simulations, it is less practical to compare two snapshots of the system at different times. Therefore, for practical reasons two copies (called “replicas”)  $\alpha$  and  $\beta$  with the same disorder but *different* initial conditions and Markov chains are simulated in parallel. The order parameter is then given by

$$q = \frac{1}{N} \sum_i S_i^\alpha S_i^\beta, \quad (33)$$

and is illustrated graphically in Fig. 11. For temperatures below  $T_c$ ,  $q$  tends to unity whereas for  $T > T_c$  on average  $q \rightarrow 0$ , similar to the magnetization for the Ising ferromagnet. Analogous to the ferromagnetic case, we can define a Binder ratio  $g$  by replacing the magnetization  $m$  with the spin overlap  $q$  to probe for the existence of a spin-glass state.

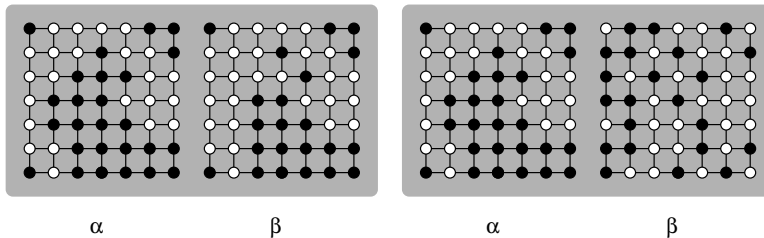


**Figure 11:** Graphical representation of the order parameter function  $q$ . Two replicas of the system  $\alpha$  and  $\beta$  with the same disorder are compared spin-by-spin. The left set corresponds to a temperature  $T \ll T_c$  where many spins agree and so  $q \rightarrow 1$  (in the depicted example  $q = 0.918$ ). The right set corresponds to  $T > T_c$ ; the spins fluctuate due to thermal fluctuations and so  $q < 1$  (here  $q = 0.408$ ).

## 6 Parallel tempering Monte Carlo

As illustrated with the case of spin glasses in Sec. 5, the free energy landscape of many-body systems with competing phases or interactions is generally characterized by many local minima that are separated by free-energy barriers. The simulation

of these systems with standard Monte Carlo [55, 59, 64] or molecular dynamics [29] methods is slowed down by long relaxation times due to the suppression of tunneling through these barriers. Already simple chemical reactions with latent heat, i.e., first-order phase transitions, present huge numerical challenges that are not present for systems which undergo second-order phase transitions where improved updating techniques, such as cluster algorithms [82, 90], can be used. For complex systems with competing interactions, one instead attempts to improve the local updating technique by introducing artificial statistical ensembles such that tunneling times through barriers are reduced and autocorrelation effects minimized.

One such method is parallel tempering Monte Carlo [5, 30, 44, 61, 81] that has proven to be a versatile “workhorse” in many fields [24]. Similar to replica Monte Carlo [81], simulated tempering [61], or extended ensemble methods [60], the algorithm aims to overcome free-energy barriers in the free energy landscape by simulating several copies of the target system at different temperatures. The system can thus escape metastable states when wandering to higher temperatures and relax to lower temperatures again in time scales several orders of magnitude smaller than for a simple Monte Carlo simulation at one fixed temperature. The method has also been combined with several other algorithms such as genetic algorithms and related optimization methods, molecular dynamics, cluster algorithms and quantum Monte Carlo.

## 6.1 Outline of the algorithm

$M$  noninteracting copies of the system are simulated in parallel at different temperatures  $\{T_1, T_2, \dots, T_M\}$ . After a fixed number of Monte Carlo sweeps (generally one lattice sweep) two copies at neighboring temperatures  $T_i$  and  $T_{i+1}$  are exchanged with a Monte Carlo like move and accepted with a probability

$$\mathcal{T}[(E_i, T_i) \rightarrow (E_{i+1}, T_{i+1})] = \min \{1, \exp[(E_{i+1} - E_i)(1/T_{i+1} - 1/T_i)]\} . \quad (34)$$

A given configuration will thus perform a random walk in temperature space overcoming free energy barriers by wandering to high temperatures where equilibration is rapid and configurations change more rapidly, and returning to low temperatures where relaxation times can be long. Unlike for simple Monte Carlo, the system can efficiently explore the complex energy landscape. Note that the update probability in Eq. (34) obeys detailed balance.

At first sight it might seem wasteful to simulate a system at multiple temperatures. In most cases, the number of temperatures does not exceed 100 values, yet the speedup attained can be 5 – 6 orders of magnitude. Furthermore, one often needs the temperature dependence of a given observable and so the method delivers data for different temperatures in one run. A simple implementation of the parallel tempering move called after a certain number of lattice sweeps using pseudo code is shown below.

```

1 algorithm parallel_tempering(*energy,*temp,*spins)
2
3   for(i = 1 ... (num_temps - 1)) do
4     delta = (1/temp[i] - 1/temp[i+1])*(energy[i] - energy[i+1])
5     if(rand(0,1) < exp(delta)) then
6       swap(spins[i],spins[i+1])
7       swap(energy[i],energy[i+1])
8     fi
9   done
    
```

The `swap( )` function swaps neighboring energies and spin configurations (`*spins`) if the move is accepted. As simple as the algorithm is, some fine tuning has to be performed for it to operate optimally.

## 6.2 Selecting the temperatures

There are *many* recipes on how to ideally select the position of the temperatures for parallel tempering Monte Carlo to perform optimally. Clearly, when the temperatures are too far apart, the energy distributions at the individual temperatures will not overlap enough and many moves will be rejected. The result is thus  $M$  independent simple Monte Carlo simulations run in parallel with no speed increase of any sort. If the temperatures are too close, CPU time is wasted.

A measure for the efficiency of a system copy to traverse the temperature space is the probability (as a function of temperature) that a swap is accepted. A good rule of thumb is to ensure that the acceptance probabilities are approximately independent of temperature, between approximately 20 – 80%, and do not show large fluctuations as these would signify the breaking-up of the random walk into segments of the temperature space. Following the aforementioned recipe, parallel tempering Monte Carlo already outperforms any simple sampling Monte Carlo method in a rough energy landscape. Still, the performance can be further increased, as outlined below.

**Traditional approaches** As mentioned before, a reasonable performance of the algorithm can be obtained when the acceptance probabilities are approximately independent of temperature. If the specific heat of a system is not strongly divergent at the phase transition—as it is the case with spin glasses—a good starting point is given by a *geometric progression* of temperatures. Given a temperature range  $[T_1, T_M]$ , the intermediate  $M - 2$  temperatures can be computed via

$$T_k = T_1 \prod_{i=1}^{k-1} R_i, \quad R_i = \sqrt[M-1]{\frac{T_M}{T_1}}. \quad (35)$$

Because relaxation is slower for lower temperatures, the geometric progression peaks the number of temperatures close to  $T_1$ . If, however, the specific heat of the system has a strong divergence, this approach is not optimal.

One can show that the acceptance probabilities are inversely correlated to the functional behavior of the specific heat per spin  $c_V$  via  $\Delta T_{i,i+1} \sim c_V T_i / \sqrt{N}$  [72].



Therefore, if  $c_V$  diverges, the acceptance probabilities for a geometric temperature set show a pronounced dip at the transition temperature. More complex methods such as the approach by Kofke [52, 53], its improvement by Rathore *et al.* [76], as well as the method suggested by Predescu *et al.* [72, 73] aim to obtain acceptance probabilities for the parallel tempering moves that are independent of temperature by compensating for the effects of the specific heat.

Finally, the number of temperatures needed can be estimated via the behavior of the specific heat. One can show that  $M \sim \sqrt{N^{1-d\nu/\alpha}}$  [44]. Here  $d$  is the space dimension,  $N$  the number of spins,  $\nu$  the critical exponent of the correlation length and  $\alpha$  the critical exponent of the specific heat.

In practice, it is straightforward to tune a temperature set produced initially via a geometric progression by adding interstitial temperatures where the acceptance rates are low. A quick simulation for only a few Monte Carlo sweeps yields enough information about the acceptance probabilities to tune the temperature set by hand without having to resort to a full equilibrium simulation.

**Improved approaches** Recently, a new iterative feedback method has been introduced to optimize the position of the temperatures in parallel tempering simulations [51]. The idea is to treat the set of temperatures as an ensemble and thus use ensemble optimization methods [86] to improve the round-trip times of a given system copy in temperature space. Unlike the conventional approaches, resources are allocated to the bottlenecks of the simulation, i.e., phase transitions and ground states where relaxation is slow. As a consequence, acceptance probabilities are temperature-dependent because more temperatures are allocated to the bottlenecks. The approach requires one to gather enough round-trip data for the temperature sets to converge and thus is not always practical. For details on the implementation, see Refs. [51] and [85], as well as Ref. [33] for an improved version.

A similar approach to optimize the efficiency of parallel tempering has recently been introduced by Bittner *et al.* [15]. Unlike the previously-mentioned feedback method, this approach leaves the position of the temperatures untouched but with an average acceptance probability of 50%. To deal with free-energy barriers in the simulation, the autocorrelation times of the simulation *without* parallel tempering have to be measured *ahead* of time. The number of MCS between parallel tempering updates is then dependent on the autocorrelation times, i.e., close to a phase transition, more MCS between parallel tempering moves are performed. Again, the method is thus optimized because resources are reallocated to where they are needed most. Unfortunately, this approach also requires a simulation to be done ahead of time to estimate the autocorrelation times, but a rough estimate is sufficient.

### 6.3 Example: Application to spin glasses

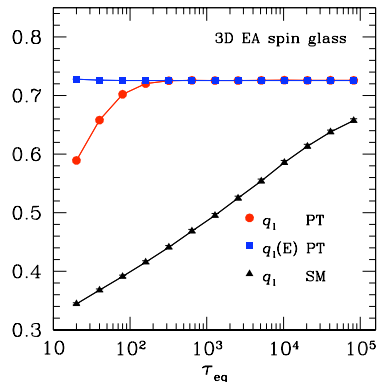
To illustrate the advantages of parallel tempering over simple Monte Carlo, we show data for a three-dimensional Ising spin glass with Normal-distributed disorder. In that case, one can use an exact relationship between the energy and a fourth-order

spin correlator known as the link overlap  $q_\ell$  [50]. The link overlap is given by

$$q_\ell = \frac{1}{dN} \sum_{\langle i,j \rangle} S_i^\alpha S_j^\alpha S_i^\beta S_j^\beta . \quad (36)$$

The sum in Eq. (36) is over neighboring spin pairs and the normalization is over all bonds. If a domain of spins in a spin glass is flipped, the link overlap measures the average length of the boundary of the domain.

**Figure 12:** Equilibration test for spin glasses with Gaussian disorder. Data for the link overlap (circles) have to equate to data for the link overlap computed from the energy (squares). This is the case after approximately 300 MCS when parallel tempering is used. A direct calculation of the link overlap using simple Monte Carlo (triangles) is not equilibrated after  $10^5$  MCS. Data for  $L = 4$ ,  $d = 3$ , 5000 samples, and  $T = 0.50$ .



The internal energy per spin  $u$  is given by

$$u = -\frac{1}{N} \sum_{\langle i,j \rangle} [J_{ij} \langle S_i S_j \rangle]_{\text{av}} , \quad (37)$$

where  $\langle \dots \rangle$  represents the Monte Carlo average for a given set of bonds, and  $[\dots]_{\text{av}}$  denotes an average over the (Gaussian) disorder. One can perform an integration by parts over  $J_{ij}$  to relate  $u$  to the average link overlap defined in Eq. (36), i.e.,

$$[\langle q_\ell \rangle]_{\text{av}} = 1 + \frac{Tu}{d} . \quad (38)$$

The simulation starts with a random spin configuration. This means that the two sides of Eq. (38) approach equilibrium from *opposite* directions. Data for  $q_\ell$  will be too small because we started from a random configuration, whereas the initial energy will not be as negative as in thermal equilibrium. Once both sides of Eq. (38) agree, the system is in thermal equilibrium. This is illustrated in Fig. 12 for the Edwards-Anderson Ising spin glass with  $4^3$  spins and  $T = 0.5$  which is approximately 50%  $T_c$ . The data are averaged over 5000 realizations of the disorder. While the data for  $q_\ell$  generated with parallel tempering Monte Carlo agree after approximately 300 MCS, the data produced with simple Monte Carlo have not reached equilibrium even after  $10^5$  MCS, thus illustrating the power of parallel tempering for systems with a rough energy landscape.

## 7 Rare events: Probing tails of energy distributions

When computing distribution functions (histograms)  $P(x)$  of a quantity  $x$  typically simple-sampling techniques are used [6]. The quantity  $x$  can be an order parameter, a free energy, an internal energy, a matching probability, etc. In these simple-sampling techniques  $N_{\text{samp}}$  instances are computed and subsequently binned in order to obtain the desired distribution. If  $N_{\text{samp}}$  samples are computed, then the maximal “resolution” of a bin is  $\sim 1/N_{\text{samp}}$ , and thus, for example,  $\sim 10^7$  samples have to be computed to resolve seven orders of magnitude in a histogram. If, however, the tails need to be probed to 18 order is magnitude precision, then the computations become quickly intractable because  $N_{\text{samp}} \sim 10^{18}$  samples have to be computed. One alternative is to use multicanonical methods [8, 11] that, for example, have been used before to overcome the limitations of simple-sampling techniques in order to probe tails of overlap distribution functions in spin glasses [9, 10].

Here we outline a method related to multicanonical approaches based on ideas presented in Ref. [35] that also overcomes the limitations of simple-sampling techniques and works for systems with disorder, e.g., spin glasses. The idea is to perform an importance-sampling simulation of  $P(x)$  *in the disorder* with a *guiding function* estimated from simple-sampling simulations. Similar approaches have been used before in the studies of distributions of sequence alignment scores [35], free-energy barriers in the Sherrington-Kirkpatrick model [14], as well as fluctuations in classical magnets [40] (albeit the latter without disorder).

### 7.1 Case study: Ground-state energy distributions

A disordered system is defined by a Hamiltonian  $\mathcal{H}_{\mathcal{J}}(\mathcal{C})$ , where the disorder configuration  $\mathcal{J}$  is chosen from a probability distribution  $\mathcal{P}(\mathcal{J})$  and  $\mathcal{C}$  denotes the phase-space configuration of the system. The ground-state energy  $E$  of a given disorder configuration  $\mathcal{J}$  is defined by

$$E(\mathcal{J}) = \min_{\mathcal{C}} \mathcal{H}_{\mathcal{J}}(\mathcal{C}). \quad (39)$$

Together with the disorder distribution  $\mathcal{P}(\mathcal{J})$ , this defines the ground-state energy distribution

$$P(E) = \int d\mathcal{J} \mathcal{P}(\mathcal{J}) \delta[E - E(\mathcal{J})]. \quad (40)$$

### 7.2 Simple sampling

$N_{\text{samp}}$  independent disorder configurations  $\mathcal{J}_i$  are chosen from  $\mathcal{P}(\mathcal{J})$  and the ground-state energy is calculated for each disorder configuration. The calculation of the ground-state energy in itself is a difficult optimization problem that we sweep under the rug (see Refs. [36, 37] for efficient methods). From the ground-state energies of these disorder configurations, the ground-state energy distribution can be estimated

via

$$P(E) = \frac{1}{N_{\text{samp}}} \sum_{i=1}^{N_{\text{samp}}} \delta [E - E(\mathcal{J}_i)], \quad (41)$$

so that the averages of functions with respect to the disorder are replaced by averages with respect to the  $N_{\text{samp}}$  random samples. The functional form of the ground-state energy distribution and its parameters can be estimated by a maximum likelihood fit of an empirical distribution  $F_\theta(E)$  with parameters  $\{\theta\}$  to the data [19]. Note that due to the limited range of energies sampled by the simple-sampling algorithm it is often difficult or even impossible to quantify how well the tails of the distribution are described by a maximum-likelihood fit.

### 7.3 Importance sampling with a guiding function

Assume it is easy to find a function  $F_\theta(E)$  that accurately describes the ground-state energy distribution calculated from a quick simple-sampling simulation as described in the previous section. In that case, an importance-sampling Monte Carlo algorithm *in the disorder* [35, 58, 68] can be used to probe the tails efficiently by using  $F_\theta(E)$  as a guiding function. We start from a random disorder configuration  $\mathcal{J} = \mathcal{J}_0$  with ground-state energy  $E(\mathcal{J}_0)$ . From the  $i$ -th configuration  $\mathcal{J}_i$ , we generate the  $i + 1$ -th configuration  $\mathcal{J}_{i+1}$  via a Metropolis-type update:

1. Select a disorder configuration  $\mathcal{J}'$  by replacing a subset of  $\mathcal{J}$  chosen at random (e.g., a single bond chosen at random) with values chosen according to  $P(\mathcal{J})$  and calculate its ground-state energy  $E(\mathcal{J}')$ .
2. Set  $\mathcal{J}_{i+1} = \mathcal{J}'$  with probability

$$P_{\text{accept}} = \min \left\{ \frac{F_\theta [E(\mathcal{J}_i)]}{F_\theta [E(\mathcal{J}')]}, 1 \right\} \quad (42)$$

and  $\mathcal{J}_{i+1} = \mathcal{J}_i$  otherwise.

With this algorithm a disorder configuration  $\mathcal{J}$  is visited with probability  $1/F_\theta[E(\mathcal{J})]$ , such that the probability to visit a disorder configuration with ground-state energy  $E$  is  $P(E)/F_\theta(E)$ . If  $F_\theta(E) \sim P(E)$ , then each energy is visited with the *same* probability resulting in a flat-histogram sampling of the ground-state energy distribution. To prevent trapping of the algorithm in an extremal region of phase space the range of energies that the algorithm is allowed to visit can be restricted (see Ref. [54] for details).

Note that successive configurations visited by the algorithm are not independent. To ensure that the data are not correlated, only samples each  $\tau$  measurements are considered in the average, where  $\tau$  is the exponential autocorrelation time of the energy. It can be computed from the energy autocorrelation function

$$\zeta_{\text{auto}}(i) = \frac{\langle E_j E_{j+i} \rangle - \langle E_j \rangle \langle E_{j+i} \rangle}{\langle E_j^2 \rangle - \langle E_j \rangle^2}, \quad (43)$$

where it decays to  $1/e$  [58]. Here  $E_i$  is the ground state energy after the  $i$ -th Monte Carlo step and  $\langle \dots \rangle$  represents an average over Monte Carlo time. To be sure that the visited ground-state configurations are not correlated, we empirically only use every  $4\tau$ -th measurement. Once the autocorrelation effects have been quantified, the data can be analyzed with the same methods as the simple-sampling results [see Eq. (41)].

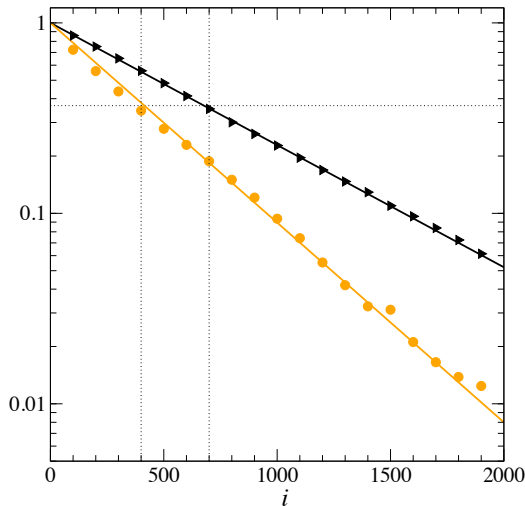


**Figure 13:** Autocorrelation function as defined in Eq. (43) for the Sherrington-Kirkpatrick spin glass and system sizes  $N = 16$  (circles) and  $N = 128$  (triangles). The value  $1/e$  is marked by the horizontal dotted line. Time steps  $i$  are measured in Monte Carlo steps. (Figure adapted from Reference [54]).

## 7.4 Example: The Sherrington-Kirkpatrick Ising spin glass

The Sherrington-Kirkpatrick [78] model is given by the Hamiltonian

$$\mathcal{H}_{\mathcal{J}}(\{S_i\}) = \sum_{i < j} J_{ij} S_i S_j, \quad (44)$$

where the  $S_i = \pm 1$  ( $i = 1, \dots, N$ ) are Ising spins, and the interactions  $\mathcal{J} = \{J_{ij}\}$  are identically and independently distributed random variables chosen from a Normal distribution with zero mean and standard deviation  $(N-1)^{-1/2}$ . The sum is over all spins in the system, i.e., the model represents the mean-field version of the Edwards-Anderson Ising spin glass introduced before.

For the SK model several optimization algorithms, such as extremal optimization [16], hysteretic optimization [69], as well as other algorithms such as genetic and Bayesian algorithms [36,37], and even parallel tempering [44] can be used to estimate ground-state energies for small to moderate system sizes.

We first compute  $10^5$  ground-state energies and bin the data into 50 bins and perform a maximum-likelihood fit to a function that describes the shape of the ground-state energy distribution best. In this case, this is a modified Gumbel distribution [32]:

$$F_{\mu,\nu,m}(E) \propto \exp \left[ m \frac{E - \mu}{\nu} - m \exp \left( \frac{E - \mu}{\nu} \right) \right]. \quad (45)$$

The modified Gumbel distribution is parametrized by the “location” parameter  $\mu$ , the “width” parameter  $\nu$ , and the “slope” parameter  $m$ . The parameters  $\mu$ ,  $\nu$  and  $m$  estimated from a maximum-likelihood fit represent the input parameters for the guiding function used in the importance-sampling simulation in the disorder. To perform a step in the Monte Carlo algorithm, we choose a site at random, replace all bonds connected to this site (the expected change in the ground-state energy is then of the order  $\sim 1/N$ ), calculate the ground-state energy of the new configuration, and accept the new configuration with the probability given in Eq. (42). A study of the energy autocorrelation shows that for system sizes between 16 and 128 spins the autocorrelation times are of the order of 400 to 700 Monte Carlo steps, see Fig. 13.

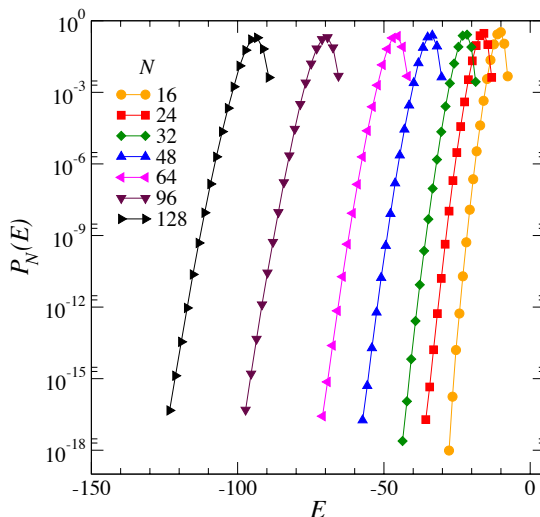


**Figure 14:** Ground-state energy distributions of the Sherrington-Kirkpatrick model for different system sizes obtained from an importance-sampling simulation with a guiding function. Although only  $\sim 10^3$  samples per system size  $N$  were simulated, the resolution of the histograms is up to 18 orders of magnitude. (Figure adapted from Reference [54]).

Figure 14 shows the energy distributions for the Sherrington-Kirkpatrick Ising spin glass for different system sizes  $N$ . The data span up to 18 orders of magnitude and were produced with approximately 1000 samples per system size, therefore illustrating the immense power of importance sampling simulations when probing tails of distributions. This would be *impossible* to obtain with simple-sampling techniques.

In comparison to similar methods [35, 40] the presented approach has several advantages due to its simplicity: Instead of iterating towards a good guiding function, which may be quite expensive computationally, we use a maximum likelihood fit as a guiding function. Therefore, the proposed algorithm is straightforward to implement and considerably more efficient than traditional approaches, provided a good guiding function, i.e., a good maximum-likelihood fit to the simple-sampling results, can be found. Note also that the method can be generalized to any distribution function, such as an order-parameter distribution.

## 8 Other Monte Carlo methods

In addition to the Monte Carlo methods outlined, there is a vast selection of other approaches based on random Monte Carlo sampling to study physical systems. In this section some selected finite-temperature Monte Carlo methods are briefly outlined. The reader is referred to the literature for details. Note that most algorithms can be combined for better performance. For example, one could combine parallel tempering with a cluster algorithm to speed up simulations both around and far below the transition.

**Cluster algorithms** In addition to the Wolff cluster algorithm [90] outlined in Sec. 4.4, the Swendsen-Wang [82] algorithm also greatly helps to overcome critical slowing down of simulations close to phase transitions. There are also specially-crafted cluster algorithms for spin glasses [41].

**Simulated annealing** Simulated annealing is probably the simplest heuristic ground-state search approach. A Monte Carlo simulation is performed until the system is in thermal equilibrium. Subsequently, the temperature is quenched according to a pre-defined protocol until  $T$  close to zero is reached. After each quench, the system is equilibrated with simple Monte Carlo. The system should converge to the ground state, although there is no guarantee that the system will not be stuck in a metastable state.

**Flat-histogram methods** Flat-histogram algorithms include the multicanonical method [8, 11], broad histograms [22] and transition matrix Monte Carlo [89] when combined with entropic sampling, as well as the adaptive algorithm of Wang and Landau [87, 88] and its improvement by Trebst *et al.* [86]. The advantage of these algorithms is that they allow for an estimate of the free energy; this is usually not available from standard Monte Carlo methods.

**Quantum Monte Carlo** In addition to the aforementioned Monte Carlo methods that treat classical problems, quantum extensions such as variational Monte Carlo, path integral Monte Carlo, etc. have been developed for quantum systems [80].

## Acknowledgments

I would like to thank Juan Carlos Andresen and Ruben Andrist for critically reading the manuscript. Furthermore, I thank M. Hasenbusch for spotting an error in Sec. 2.1.

## References

- [1] The bulk of this chapter is based on material collected from the different books cited.
- [2] The alcohol is to improve the randomness of the sampling. If the experimentalist is not of legal drinking age, it is recommended to close the eyes and rotate 42 times on the spot at high speed before a pebble is thrown.
- [3] The pseudo code used does not follow any rules and is by no means consistent. But it should bring the general ideas across.
- [4] Although the algorithm is known as the *Metropolis algorithm*, N. Metropolis' contribution to the project was minimal. He merely was the team leader at the lab. The bulk of the work was carried out by two couples, the Rosenbluths and the Tellers.
- [5] The method is also known under the name of "Exchange Monte Carlo" (EMC) and "Multiple Markov Chain Monte Carlo" (MCMC).
- [6] This section is based on work published in Ref. [54].
- [7] H. G. Ballesteros, A. Cruz, L. A. Fernandez, V. Martin-Mayor, J. Pech, J. J. Ruiz-Lorenzo, A. Tarancon, P. Tellez, C. L. Ullod, and C. Ungil. Critical behavior of the three-dimensional Ising spin glass. *Phys. Rev. B*, 62:14237, 2000.
- [8] B. Berg and T. Neuhaus. Multicanonical ensemble: a new approach to simulate first-order phase transitions. *Phys. Rev. Lett.*, 68:9, 1992.
- [9] B. A. Berg, A. Billoire, and W. Janke. Functional form of the Parisi overlap distribution for the three-dimensional Edwards-Anderson Ising spin glass. *Phys. Rev. E*, 65:045102, 2002.
- [10] B. A. Berg, A. Billoire, and W. Janke. Overlap distribution of the three-dimensional Ising model. *Phys. Rev. E*, 66:046122, 2002.
- [11] B. A. Berg and T. Neuhaus. Multicanonical algorithms for first order phase transitions. *Phys. Lett. B*, 267:249, 1991.
- [12] K. Binder. Critical properties from Monte Carlo coarse graining and renormalization. *Phys. Rev. Lett.*, 47:693, 1981.
- [13] K. Binder and A. P. Young. Spin glasses: Experimental facts, theoretical concepts and open questions. *Rev. Mod. Phys.*, 58:801, 1986.



- 
- [14] E. Bittner and W. Janke. Free-Energy Barriers in the Sherrington-Kirkpatrick Model. *Europhys. Lett.*, 74:195, 2006.
- [15] E. Bittner, A. Nußbaumer, and W. Janke. Make life simple: Unleash the full power of the parallel tempering algorithm. *Phys. Rev. Lett.*, 101:130603, 2008.
- [16] S. Boettcher and A. G. Percus. Optimization with Extremal Dynamics. *Phys. Rev. Lett.*, 86:5211, 2001.
- [17] Y. Cannella and J. A. Mydosh. Magnetic ordering in gold-iron alloys (susceptibility and thermopower studies). *Phys. Rev. B*, 6:4220, 1972.
- [18] J. Cardy. *Scaling and Renormalization in Statistical Physics*. Cambridge University Press, Cambridge, 1996.
- [19] G. Cowan. *Statistical Data Analysis*. Oxford Science Publications, New York, 1998.
- [20] J. R. L. de Almeida and D. J. Thouless. Stability of the Sherrington-Kirkpatrick solution of a spin glass model. *J. Phys. A*, 11:983, 1978.
- [21] C. de Dominicis and I. Giardinà. *Random Fields and Spin Glasses*. Cambridge University Press, Cambridge, 2006.
- [22] P. M. C. de Oliveira, T. J. P. Penna, and H. J. Herrmann. Broad Histogram Method. *Braz. J. Phys.*, 26:677, 1996.
- [23] H. T. Diep. *Frustrated Spin Systems*. World Scientific, Singapore, 2005.
- [24] D. J. Earl and M. W. Deem. Parallel Tempering: Theory, Applications, and New Perspectives. *Phys. Chem. Chem. Phys.*, 7:3910, 2005.
- [25] S. F. Edwards and P. W. Anderson. Theory of spin glasses. *J. Phys. F: Met. Phys.*, 5:965, 1975.
- [26] D. S. Fisher and D. A. Huse. Ordered phase of short-range Ising spin-glasses. *Phys. Rev. Lett.*, 56:1601, 1986.
- [27] D. S. Fisher and D. A. Huse. Absence of many states in realistic spin glasses. *J. Phys. A*, 20:L1005, 1987.
- [28] K. H. Fisher and J. A. Hertz. *Spin Glasses*. Cambridge University Press, Cambridge, 1991.
- [29] D. Frenkel and B. Smit. *Understanding Molecular Simulation*. Academic Press, New York, 1996.
- [30] C. Geyer. Monte Carlo Maximum Likelihood for Dependent Data. In E. M. Keramidas, editor, *23rd Symposium on the Interface*, page 156, Fairfax Station, 1991. Interface Foundation.

- [31] N. Goldenfeld. *Lectures On Phase Transitions And The Renormalization Group*. Westview Press, Jackson, 1992.
- [32] E. J. Gumbel. Multivariate Extremal Distributions. *Bull. Inst. Internat. de Statistique*, 37:471, 1960.
- [33] F. Hamze, N. Dickson, and K. Karimi. Robust parameter selection for parallel tempering. (*arXiv:cond-mat/1004.2840*), 2010.
- [34] A. K. Hartmann. Scaling of stiffness energy for three-dimensional  $\pm J$  Ising spin glasses. *Phys. Rev. E*, 59:84, 1999.
- [35] A. K. Hartmann. Sampling rare events: Statistics of local sequence alignments. *Phys. Rev. E*, 65:056102, 2002.
- [36] A. K. Hartmann and H. Rieger. *Optimization Algorithms in Physics*. Wiley-VCH, Berlin, 2001.
- [37] A. K. Hartmann and H. Rieger. *New Optimization Algorithms in Physics*. Wiley-VCH, Berlin, 2004.
- [38] A. K. Hartmann and A. P. Young. Lower critical dimension of Ising spin glasses. *Phys. Rev. B*, 64:180404(R), 2001.
- [39] G. Hed, A. P. Young, and E. Domany. Lack of Ultrametricity in the Low-Temperature phase of 3D Ising Spin Glasses. *Phys. Rev. Lett.*, 92:157201, 2004.
- [40] R. Hilfer, B. Biswal, H. G. Mattutis, and W. Janke. Multicanonical Monte Carlo study and analysis of tails for the order-parameter distribution of the two-dimensional Ising model. *Phys. Rev. E*, 68:046123, 2003.
- [41] J.J. Houdayer. A cluster Monte Carlo algorithm for 2-dimensional spin glasses. *Eur. Phys. J. B.*, 22:479, 2001.
- [42] J.J. Houdayer, F. Krzakala, and O. C. Martin. Large-scale low-energy excitations in 3-d spin glasses. *Eur. Phys. J. B.*, 18:467, 2000.
- [43] K. Huang. *Statistical Mechanics*. Wiley, New York, 1987.
- [44] K. Hukushima and K. Nemoto. Exchange Monte Carlo method and application to spin glass simulations. *J. Phys. Soc. Jpn.*, 65:1604, 1996.
- [45] E. Ising. Beitrag zur Theorie des Ferromagnetismus. *Z. Phys.*, 31:253, 1925.
- [46] S. Jimenez, V. Martin-Mayor, and S. Perez-Gaviro. Rejuvenation and memory in model spin glasses in 3 and 4 dimensions. *Phys. Rev. B*, 72:054417, 2005.
- [47] K. Jonason, E. Vincent, J. Hammann, J. P. Bouchaud, and P. Nordblad. Memory and Chaos Effects in Spin Glasses. *Phys. Rev. Lett.*, 81:3243, 1998.

- 
- [48] H. G. Katzgraber and A. K. Hartmann. Ultrametricity and Clustering of States in Spin Glasses: A One-Dimensional View. *Phys. Rev. Lett.*, 102:037207, 2009.
- [49] H. G. Katzgraber, M. Körner, and A. P. Young. Universality in three-dimensional Ising spin glasses: A Monte Carlo study. *Phys. Rev. B*, 73:224432, 2006.
- [50] H. G. Katzgraber, M. Palassini, and A. P. Young. Monte Carlo simulations of spin glasses at low temperatures. *Phys. Rev. B*, 63:184422, 2001.
- [51] H. G. Katzgraber, S. Trebst, D. A. Huse, and M. Troyer. Feedback-optimized parallel tempering Monte Carlo. *J. Stat. Mech.*, P03018, 2006.
- [52] D. A. Kofke. Comment on "The incomplete beta function law for parallel tempering sampling of classical canonical systems" [*J. Chem. Phys.* 120, 4119 (2004)]. *J. Chem. Phys.*, 121:1167, 2004.
- [53] D. A. Kofke. On the acceptance probability of replica-exchange Monte Carlo trials. *J. Chem. Phys.*, 117:6911, 2004.
- [54] M. Körner, H. G. Katzgraber, and A. K. Hartmann. Probing tails of energy distributions using importance-sampling in the disorder with a guiding function. *J. Stat. Mech.*, P04005, 2006.
- [55] W. Krauth. Introduction To Monte Carlo Algorithms. In J. Kertesz and I. Kondor, editors, *Advances in Computer Simulation*. Springer Verlag, Heidelberg, 1998.
- [56] W. Krauth. *Algorithms and Computations*. Oxford University Press, New York, 2006.
- [57] F. Krzakala and O. C. Martin. Spin and link overlaps in 3-dimensional spin glasses. *Phys. Rev. Lett.*, 85:3013, 2000.
- [58] D. P. Landau and K. Binder. *A Guide to Monte Carlo Simulations in Statistical Physics*. Cambridge University Press, 2000.
- [59] R. H. Landau and M. J. Páez. *Computational Physics*. Wiley, New York, 1997.
- [60] A. P. Lyubartsev, A. A. Martsinovski, S. V. Shevkunov, and P. N. Vorontsov-Velyaminov. New approach to Monte Carlo calculation of the free energy: Method of expanded ensembles. *J. Chem. Phys.*, 96:1776, 1992.
- [61] E. Marinari and G. Parisi. Simulated tempering: A new Monte Carlo scheme. *Europhys. Lett.*, 19:451, 1992.
- [62] E. Marinari and G. Parisi. On the effects of changing the boundary conditions on the ground state of Ising spin glasses. *Phys. Rev. B*, 62:11677, 2000.

- [63] N. Metropolis, A. W. Rosenbluth, M. N. Rosenbluth, A. H. Teller, and E. Teller. Equation of State Calculations by Fast Computing Machines. *J. Chem. Phys.*, 21:1087, 1953.
- [64] N. Metropolis and S. Ulam. The Monte Carlo Method. *J. Am. Stat. Assoc.*, 44:335, 1949.
- [65] M. Mézard, G. Parisi, and M. A. Virasoro. *Spin Glass Theory and Beyond*. World Scientific, Singapore, 1987.
- [66] C. Newman and D. L. Stein. Non-mean-field behavior of realistic spin glasses. *Phys. Rev. Lett.*, 76:515, 1996.
- [67] C. M. Newman and D. L. Stein. Short-range spin glasses: Results and speculations. In *Lecture Notes in Mathematics 1900*, page 159. Springer-Verlag, Berlin, 2007. (cond-mat/0503345).
- [68] M. E. J. Newman and G. T. Barkema. *Monte Carlo Methods in Statistical Physics*. Oxford University Press Inc., New York, USA, 1999.
- [69] K. F. Pal. Hysteretic optimization for the Sherrington-Kirkpatrick spin glass. *Physica A*, 367:261, 2006.
- [70] M. Palassini and S. Caracciolo. Universal Finite-Size Scaling Functions in the 3D Ising Spin Glass. *Phys. Rev. Lett.*, 82:5128, 1999.
- [71] M. Palassini and A. P. Young. Nature of the spin glass state. *Phys. Rev. Lett.*, 85:3017, 2000.
- [72] C. Predescu, M. Predescu, and C.V. Ciobanu. The incomplete beta function law for parallel tempering sampling of classical canonical systems. *J. Chem. Phys.*, 120:4119, 2004.
- [73] C. Predescu, M. Predescu, and C.V. Ciobanu. On the Efficiency of Exchange in Parallel Tempering Monte Carlo Simulations. *J. Phys. Chem. B*, 109:4189, 2005.
- [74] W. H. Press, S. A. Teukolsky, W. T. Vetterling, and B. P. Flannery. *Numerical Recipes in C*. Cambridge University Press, Cambridge, 1995.
- [75] V. Privman, editor. *Finite Size Scaling and Numerical Simulation of Statistical Systems*. World Scientific, Singapore, 1990.
- [76] N. Rathore, M. Chopra, and J. J. de Pablo. Optimal allocation of replicas in parallel tempering simulations. *J. Chem. Phys.*, 122:024111, 2005.
- [77] L. Reichl. *A Modern Course in Statistical Physics*. Wiley, New York, 1998.
- [78] D. Sherrington and S. Kirkpatrick. Solvable model of a spin glass. *Phys. Rev. Lett.*, 35:1792, 1975.

- 
- [79] H. E. Stanley. *An Introduction to Phase Transitions and Critical Phenomena*. Oxford University Press, Oxford, 1971.
- [80] M. Suzuki. *Quantum Monte Carlo Methods in Condensed Matter Physics*. World Scientific, Singapore, 1993.
- [81] R. H. Swendsen and J. Wang. Replica Monte Carlo simulation of spin-glasses. *Phys. Rev. Lett.*, 57:2607, 1986.
- [82] R. H. Swendsen and J. Wang. Nonuniversal critical dynamics in Monte Carlo simulations. *Phys. Rev. Lett.*, 58:86, 1987.
- [83] M. Talagrand. *Spin glasses: a Challenge for Mathematicians*. Springer, Berlin, 2003.
- [84] M. Talagrand. The Parisi formula. *Ann. of Math.*, 163:221, 2006.
- [85] S. Trebst, D. A. Huse, E. Gull, H. G. Katzgraber, U. H. E. Hansmann, and M. Troyer. Computer Simulation Studies in Condensed Matter Physics XIX. In D. P. Landau, S. P. Lewis, and H.-B. Schüttler, editors, *Ensemble optimization techniques for the simulation of slowly equilibrating systems*, volume 115. Springer, Berlin, 2007.
- [86] S. Trebst, D. A. Huse, and M. Troyer. Optimizing the ensemble for equilibration in broad-histogram Monte Carlo simulations. *Phys. Rev. E*, 70:046701, 2004.
- [87] F. Wang and D. P. Landau. Determining the density of states for classical statistical models: A random walk algorithm to produce a flat histogram. *Phys. Rev. E*, 64:056101, 2001.
- [88] F. Wang and D. P. Landau. An efficient, multiple-range random walk algorithm to calculate the density of states. *Phys. Rev. Lett.*, 86:2050, 2001.
- [89] J.-S. Wang and R. H. Swendsen. Transition Matrix Monte Carlo Method. *J. Stat. Phys.*, 106:245, 2002.
- [90] U. Wolff. Collective Monte Carlo updating for spin systems. *Phys. Rev. Lett.*, 62:361, 1989.
- [91] J. M. Yeomans. *Statistical Mechanics of Phase Transitions*. Oxford University Press, Oxford, 1992.
- [92] A. P. Young, editor. *Spin Glasses and Random Fields*. World Scientific, Singapore, 1998.
- [93] A. P. Young and H. G. Katzgraber. Absence of an Almeida-Thouless line in Three-Dimensional Spin Glasses. *Phys. Rev. Lett.*, 93:207203, 2004.